Massive Dirac particles on the background of charged de Sitter black hole manifolds

F. Belgiorno[*]

Dipartimento di Fisica, Università di Milano, 20133 Milano, Italy,
and I.N.F.N., Sezione di Milano, Italy

S. L. Cacciatori[†]

Dipartimento di Fisica e Matematica, Università dell'Insubria, 22100 Como, Italy,
and I.N.F.N., Sezione di Milano, Italy

We consider the behavior of massive Dirac fields on the background of a charged de Sitter black hole. All black hole geometries are taken into account, including the Reissner-Nordström-de Sitter one, the Nariai case, and the ultracold case. Our focus is at first on the existence of bound quantum mechanical states for the Dirac Hamiltonian on the given backgrounds. In this respect, we show that in all cases no bound state is allowed, which amounts also to the nonexistence of normalizable time-periodic solutions of the Dirac equation. This quantum result is in contrast to classical physics, and it is shown to hold true even for extremal cases. Furthermore, we shift our attention on the very interesting problem of the quantum discharge of the black holes. Following the Damour-Deruelle-Ruffini approach, we show that the existence of level crossing between positive and negative continuous energy states is a signal of the quantum instability leading to the discharge of the black hole, and in the cases of the Nariai geometry and of the ultracold geometries we also calculate in WKB approximation the transmission coefficient related to the discharge process.

I. INTRODUCTION

Black holes in de Sitter (dS) space are an interesting subject of investigation, both on the theoretical side and on the experimental one. On one hand, the contextual presence of a black hole event horizon and of a cosmological event horizon, to be associated with the corresponding quantum emission of thermal radiation [1] is a feature which enriches the framework of black hole thermodynamics in itself and also because of the possibility to obtain a true nonequilibrium situation when two different temperatures coexist on the same manifold. On the other hand, black hole physics in space-times with a positive cosmological constant appear to be of direct physical interest, because the present-day measurements of cosmological parameters confirm the presence of a small positive cosmological constant, which implies that dS backgrounds are the real black hole backgrounds to be taken into account for physical considerations. In this paper, we consider some relevant aspects of the physics of massive quantum Dirac particles on dS black hole backgrounds. We first show that, as expected, the Dirac Hamiltonian is well behaved in the sense that its self-adjointness can be ensured without imposing any boundary condition. We also determine, by means of spectral analysis, two relevant physical properties: there is no mass gap in the spectrum, even if the particles are massive, and there exists no

quantum bound state for charged particles around a charged black hole, in contrast to classical physics. The latter property amounts to the absence of normalizable and time-periodic solutions of the Dirac equation on the background of a nonextremal Reissner-Nordström-dS black hole, in full agreement with the recent literature on this topic [2–6]. Furthermore, we show that this holds true also in the extremal case, due to the prominent role of the cosmological event horizon, as well as in the so-called Nariai case and in the ultracold ones.

In the second part of the paper, we also take into account the problem of pair creation by a charged black hole. This is a long-standing topic in the framework of quantum effects in the field of a black hole, as old as the Hawking effect but still different in its origin [7,8]. The latter can be brought back to vacuum instability in the presence of an external field (see e.g. [9,10] and, in the recent literature [11–13]). It is shown that the presence of level crossing, i.e. of overlap between positive continuum energy states and negative continuum energy ones, according to a criterion introduced by Ruffini, Damour, and Deruelle [14–17], recently extended to include the Reissner-Nordström–anti-dS (RN-AdS) case [18], is a still valid tool for investigating pair creation of charged Dirac particles even in presence of a positive cosmological constant. We point out that this method is equivalent to the ones commonly exploited in order to investigate instability properties of the vacuum [11,13], even if the criterion of level crossing seems to be specific of the above references [14–17].

---
[*]belgiorno@mi.infn.it
[†]sergio.cacciatori@uninsubria.it

Special attention is focused on special cases, like the Nariai and the ultracold ones, for which an estimate in WKB approximation of the transmission coefficient related to the process of pair-creation is provided.

This work, together with the analogous one concerning the Dirac equation on the background of a Reissner-Nordström-AdS black hole, completes the analysis of the process of pair creation by a charged black hole in the presence of a cosmological constant, and in this sense it also extends the analysis on the background of a Reissner-Nordström black hole [7,8]. We recall that, in spite of the fact that dS and AdS differ for a change of sign in the cosmological constant, very different manifolds and very different physics occur on these backgrounds. We mention, for example, the occurrence of closed timelike curves in the AdS case, a problem which can be overcome by passing to the universal covering, but at the price to deal with the lack of global hyperbolicity [19]. On the quantum level, self-adjointness of the wave operators cannot be ensured in general (see e.g. [18] for RN-AdS black holes), and boundary conditions have to be introduced for some cases, because of a boundarylike behavior of the AdS asymptotic region. In particular, for $\mu\sqrt{\frac{3}{|\Lambda|}} < \frac{1}{2}$, where μ is the Dirac particle mass and Λ is the (negative) cosmological constant, several boundary conditions can be chosen (see e.g. [20] for explicit choices of boundary conditions for the Dirac Hamiltonian on pure AdS), and then physics is not uniquely defined.

In the dS cases we discuss herein, no such features arise. Moreover, black holes are characterized by a single event horizon in the AdS case and by two event horizons in the dS one. This fact is shown to be at the root of the fact that in the de Sitter case there is always level crossing, which is in contrast not only to the AdS case but also with the standard RN case ($\Lambda = 0$). This feature is then peculiar of these solutions; notwithstanding, the actual presence of pair creation is to be associated with further conditions, to be related with the actual largeness of the forbidden region separating positive energy states from negative energy ones. For completeness, we recall that charged Dirac fields in the more general Kerr-Newman-de Sitter background have been studied with the aim to determine their quasinormal modes in [21].

II. DIRAC HAMILTONIAN IN THE CASE $r_+ < r_c$: REISSNER-NORDSTRÖM-DS BLACK HOLES

We first define the one-particle Hamiltonian for Dirac massive particles on the Reissner-Nordström-dS black hole geometry (RN-dS black hole in the following). We use natural units $\hbar = c = G = 1$ and unrationalized electric units. The metric of the RN-dS black hole manifold ($t \in \mathbb{R}$; $r \in (r_+, r_c)$; $\Omega \in S^2$) is

$$ds^2 = -f(r)dt^2 + \frac{1}{f(r)}dr^2 + r^2 d\Omega^2$$

$$f(r) = 1 - \frac{2M}{r} + \frac{Q^2}{r^2} - \frac{\Lambda}{3}r^2; \tag{1}$$

M is the mass and Q is the electric charge of the black hole, and $\Lambda > 0$ is the cosmological constant; let us define $L = \sqrt{\frac{3}{\Lambda}}$; the equation $f(r) = 0$ is assumed to admit solutions $r_c > r_+ \geq r_- > r_0$; then one obtains

$$f(r) = \frac{1}{L^2 r^2}(r_c - r)(r - r_+)(r - r_-)(r - r_0). \tag{2}$$

r_c is the radius of the cosmological horizon, r_+ is the radius of the black hole event horizon, and r_- is the radius of the Cauchy horizon. Moreover, due to the actual lack of a term proportional to r^3, one has $r_0 = -(r_c + r_+ + r_-)$. The above reparametrization of the metric amounts to implementing the following relations between r_c, r_+, r_- and M, Q, L:

$$L^2 = r_c(r_+ + r_- + r_c) + r_+^2 + r_-^2 + r_+ r_-$$

$$2L^2 M = r_c^2 r_+ + r_c r_+^2 + 2r_c r_+ r_- + r_c^2 r_- + r_c r_-^2$$
$$+ r_+^2 r_- + r_+ r_-^2$$

$$L^2 Q^2 = r_c r_+ r_-(r_c + r_+ + r_-).$$

It is not difficult to show that four real zeros of $f(r) = 0$ exist (and three are positive) if and only if the following conditions are implemented:

$$0 < Q^2 < \frac{L^2}{12} \tag{3}$$

$$M_{\text{extr}} \leq M < M_{\text{max}}, \tag{4}$$

where

$$M_{\text{extr}} = \frac{L}{3\sqrt{6}}\sqrt{1 - \sqrt{1 - 12\frac{Q^2}{L^2}}}\left(2 + \sqrt{1 - 12\frac{Q^2}{L^2}}\right) \tag{5}$$

is the mass of the extremal black hole with $r_- = r_+$, and

$$M_{\text{max}} = \frac{L}{3\sqrt{6}}\sqrt{1 + \sqrt{1 - 12\frac{Q^2}{L^2}}}\left(2 - \sqrt{1 - 12\frac{Q^2}{L^2}}\right) \tag{6}$$

is the mass of the black hole with $r_+ = r_c$ (see Sec. IV). See [22] for the analysis of the more general Kerr-Newman-dS case.

The vector potential associated with the RN-dS solution is $A_\mu = (-Q/r, 0, 0, 0)$. Spherical symmetry, as usual, allows one to separate variables [23–26] and to obtain the following reduced Hamiltonian:

$$H_{\text{red}} = \begin{bmatrix} -\sqrt{f}\mu + \frac{eQ}{r} & f\partial_r + k\frac{\sqrt{f}}{r} \\ -f\partial_r + k\frac{\sqrt{f}}{r} & \sqrt{f}\mu + \frac{eQ}{r} \end{bmatrix}, \tag{7}$$

where $f(r)$ is the same as in (1), $k = \pm(j + 1/2) \in \mathbb{Z} - \{0\}$ is the angular momentum eigenvalue and μ is the mass of the Dirac particle. The Hilbert space in which H_{red} is formally defined is the Hilbert space $L^2[(r_+, r_c), 1/f(r)dr]^2$ of the two-dimensional vector functions $\vec{g} \equiv \binom{g_1}{g_2}$ such that

$$\int_{r_+}^{r_c} \frac{dr}{f(r)} (|g_1(r)|^2 + |g_2(r)|^2) < \infty.$$

As a domain for the minimal operator associated with H_{red} we can choose the following subset of $L^2[(r_+, r_c), 1/f(r)dr]^2$: the set $C_0^\infty(r_+, r_c)^2$ of the two-dimensional vector functions $\vec{g}$ whose components are smooth and of compact support [27]. It is useful to define a new tortoise-like variable y:

$$\frac{dy}{dr} = \frac{1}{f(r)} \tag{8}$$

and then one obtains $y \in \mathbb{R}$, with $y \to \infty \Leftrightarrow r \to r_c^-$ and $y \to -\infty \Leftrightarrow r \to r_+^+$. The reduced Hamiltonian becomes

$$H_{\text{red}} = D_0 + V(y), \tag{9}$$

where

$$D_0 = \begin{bmatrix} 0 & \partial_y \\ -\partial_y & 0 \end{bmatrix}$$

and

$$V(r(y)) = \begin{bmatrix} -\sqrt{f}\mu + \frac{eQ}{r} & k\frac{\sqrt{f}}{r} \\ k\frac{\sqrt{f}}{r} & \sqrt{f}\mu + \frac{eQ}{r} \end{bmatrix}.$$

The Hilbert space of interest for the Hamiltonian (9) is $L^2[\mathbb{R}, dy]^2$. We check if the one-particle Hamiltonian is well defined in the sense that no boundary conditions are required in order to obtain a self-adjoint operator. This means that we have to check if the reduced Hamiltonian is essentially self-adjoint; with this aim, we check if the solutions of the equation

$$H_{\text{red}}\vec{g} = \lambda\vec{g} \tag{10}$$

are square integrable in a right neighborhood of $y = -\infty$ and in a left neighborhood of $y = +\infty$. The so-called Weyl alternative generalized to a system of first order ordinary differential equations ([27], theorem 5.6) can be applied, in particular, if in a right neighborhood of $y = -\infty$ at least one solution not square integrable exists for every $\lambda \in \mathbb{C}$, then no boundary condition is required and the so-called limit point case (LPC) is verified; if instead for every $\lambda \in \mathbb{C}$ all the solutions of $(H_{\text{red}} - \lambda)\vec{g} = 0$ lie in $L^2[(-\infty, c), dy]^2$, with $-\infty < c < \infty$, the so-called limit circle case occurs (and boundary conditions are required). Analogously, one studies the behavior of solutions in a left neighborhood of $y = \infty$. The Hamiltonian operator is essentially self-adjoint if the LPC is verified both at $y = -\infty$

and at $y = \infty$ (cf. [27], theorem 5.7). In the case at hand, we can refer to the corollary to theorem 6.8 (page 99) of [27], both for $y \to -\infty$ and for $y \to \infty$. Thus, the Dirac operator defined on $C_0^\infty(r_+, r_c)^2$ is essentially self-adjoint on the RN-dS black hole background.

III. QUALITATIVE SPECTRAL PROPERTIES AND TIME-PERIODIC SOLUTIONS IN THE CASE $r_+ < r_c$

We first show that the essential spectrum of the unique self-adjoint extension of the Dirac Hamiltonian (still indicated with H_{red}) coincides with $\mathbb{R}$ both in the case of nonextremal black holes and in the extremal case. This feature is expected in the presence of a black hole horizon and is well known in the case of scalar particles [28], and also verified in the case of Dirac particles on Kerr-Newman black hole manifold (see e.g. [29,30]). We confirm that it is verified also in the present cases. From a physical point of view, it also implies that there is no room for isolated eigenvalues, and then that there is no "standard" bound state (in the sense that a charged particle with charge opposite to the charge of the black hole cannot form a bound state which is analogous to the bound state an electron forms around an atomic nucleus). Moreover, a finer analysis allows also to conclude that, both in the nonextremal case and in the extremal one, the point spectrum is empty, and then no quantum bound state, i.e. no possibility to obtain a normalizable time-periodic solution of the Dirac equation, exists.

A. Essential spectrum

One expects that, in the presence of an event horizon, i.e. of a so-called ergosurface, the mass gap vanishes and that the continuous spectrum includes the whole real line. We recall that qualitative spectral methods for the Dirac equation (see e.g. [26,27]) have been applied to Dirac fields on a black hole background in [4,29]. In order to verify this property, we adopt the decomposition method [27]. We split the interval (r_+, r_c) at an inner point r_1 and then consider the formal differential expression (7) restricted to the subintervals $(r_+, r_1]$ and $[r_1, r_c)$. Roughly speaking, we refer to the aforementioned expressions as the "restriction of the Hamiltonian H_{red} to the interval $(r_+, r_1]$ and to the interval $[r_1, r_c)$" and write e.g. $H_{\text{red}}|_{[r_1, r_c)}$ for the latter. We limit ourselves to consider the latter restriction, which is relative to the novel feature of space-time, with respect to previously discussed cases, represented by the cosmological horizon. In the tortoiselike coordinate y, one finds a potential P such that

$$P = \begin{bmatrix} -\sqrt{f}\mu + \frac{eQ}{r} & k\frac{\sqrt{f}}{r} \\ k\frac{\sqrt{f}}{r} & \sqrt{f}\mu + \frac{eQ}{r} \end{bmatrix}$$

and it holds

$$\lim_{y \to \infty} P(y) = P_0 = \begin{bmatrix} \Phi_c & 0 \\ 0 & \Phi_c \end{bmatrix}$$

which is in diagonal form and whose eigenvalues coincide. We apply theorem 16.6, page 249 of Ref. [27], which implies that, if ν_-, ν_+, with $\nu_- \leq \nu_+$, are the eigenvalues of the matrix P_0, then $\{\mathbb{R} - (\nu_-, \nu_+)\} \subset \sigma_e(H_{\text{red}}|_{[y(r_1),\infty)})$ if

$$\lim_{y \to \infty} \frac{1}{y} \int_{\epsilon_0}^{y} dt |P(t) - P_0| = 0, \tag{11}$$

where $|\cdot|$ stays for any norm in the set of 2×2 matrices (we choose the Euclidean norm). In our case one has to find the limit as $y \to \infty$ for the following expression:

$$\frac{1}{y} \int_{r_1}^{r(y)} dr \frac{1}{h(r)} \frac{1}{\sqrt{r_c - r}}$$
$$\times \sqrt{2\mu^2 h(r) + 2(\Phi_+^2(r_c - r) + k^2 h(r)) \frac{1}{r^2}}, \tag{12}$$

where we put $h(r) = \frac{f(r)}{r_c - r}$. Both in the nonextremal case and in the extremal one, the above integral is finite as $r \to r_c$, i.e. as $y \to \infty$, and then the limit is zero (We recall that the difference between the nonextremal case and the extremal one from this point occurs when studying the limit as $r \to r_+$, i.e. as $y \to -\infty$. In the extremal case $r_+ = r_-$, the corresponding integral diverges but a trivial use of the l'Hospital's rule allows one to find that the aforementioned limit is still zero.) As a consequence, we can state that

$$\sigma_e(H_{\text{red}}) = \mathbb{R}. \tag{13}$$

A completely analogous conclusion can be stated for the restriction to $(-\infty, r_1)$, and again the essential spectrum contribution one finds is $\mathbb{R}$ both in the nonextremal case and in the extremal one.

B. Absence of states of the point spectrum

Qualitative spectral analysis of the reduced Hamiltonian in the nonextremal case can be implemented by means of theorems in [31] or also in [27]. In [22] a proof was given for the more general case of the Dirac equation in a Kerr-Newman-de Sitter black hole background, again in the case $r_+ < r_c$. For the sake of completeness, we sketch the strategy and also provide some details involving some differences with respect to [22].

We note that, given a decomposition point $r_1 \in (r_+, r_c)$, we can introduce the following self-adjoint operators H_{hor} and H_c on the respective domains $D(H_{\text{hor}}) = \{\vec{g} \in L^2[(r_+, r_1), 1/f(r)dr]^2; \vec{g}$ is locally absolutely continuous; $g_1(r_1) = 0; H_{\text{hor}}\vec{g} \in L^2[(r_+, r_1), 1/f(r)dr]^2\}$, and analogously $D(H_c) = \{\vec{g} \in L^2[(r_1, r_c), 1/f(r)dr]^2, \vec{g}$ is locally absolutely continuous; $g_1(r_1) = 0; H_c\vec{g} \in L^2[(r_1, r_c), 1/f(r)dr]^2\}$. According to the decomposition method applied to the absolutely continuous spectrum, one has $\sigma_{ac}(H_{\text{red}}) = \sigma_{ac}(H_{\text{hor}}) \cup \sigma_{ac}(H_c)$ (cf. e.g. [22]). Theorem

16.7 in [27] allows one to conclude that, in the nonextremal case, H_{hor} has an absolutely continuous spectrum in $\mathbb{R} - \Phi_+$, where $\frac{\Phi_+}{e}$ is the electrostatic potential at the black hole event horizon, and that H_c has an absolutely continuous spectrum in $\mathbb{R} - \Phi_c$, where $\frac{\Phi_c}{e}$ is the electrostatic potential at the cosmological horizon. Moreover, for $eQ > 0$ it has to hold $\Phi_c < \Phi_+$, and $\Phi_c > \Phi_+$ for $eQ < 0$, due to the inequality $r_c > r_+$. In any case, $\Phi_c \neq \Phi_+$ occurs, and this is an interesting fact in the light of the study of the pair-creation process, as we shall see in the following section. As to the spectral properties of the reduced Hamiltonian, one can easily infer that the spectrum is absolutely continuous in $\mathbb{R}$ (indeed, the above analysis allows one to conclude that the spectrum is absolutely continuous in $\mathbb{R} - \{\{\Phi_c\} \cap \{\Phi_+\}\}$ but of course the latter set coincides with $\mathbb{R}$). As to the extremal case, one can again refer to theorem 16.7 in [27] for H_c and to theorem 1 in [31] for H_{hor} to conclude that the spectrum is absolutely continuous in $\mathbb{R} - \{\{\Phi_c\} \cap \{\Phi_+\}\}$. Again, the latter set is $\mathbb{R}$.

IV. NARIAI SOLUTION

We take into consideration the special case of the so-called charged Nariai solution [32,33], which is a black hole solution with $r_- < r_+ = r_c$. As known, the metric (1) is no more valid and a suitable transformation is necessary. It can be shown that the manifold can be described by

$$ds^2 = \frac{1}{A}(-\sin^2(\chi)d\psi^2 + d\chi^2) + \frac{1}{B}(d\theta^2 + \sin^2(\theta)d\phi^2) \tag{14}$$

with $\psi \in \mathbb{R}$, $\chi \in (0, \pi)$, and where $B = \frac{1}{2Q^2} \times (1 - \sqrt{1 - 12\frac{Q^2}{L^2}})$ and $A = \frac{6}{L^2} - B$ are constants such that $\frac{A}{B} < 1$ [32,33]. We note that there is no warping factor in the metric between the "radial" part and the S^2 part. For an electrically charged black hole, we can choose $A_i = -Q\frac{B}{A}\cos(\chi)\delta_i^0$. We study the Dirac equation as in [23,24]. With the same notation as in [23], we introduce the so-called generalized Dirac matrices such that $\{\gamma_i, \gamma_j\} = 2g_{ij}$:

$$\gamma_0 = \frac{\sin(\chi)}{\sqrt{A}}\tilde{\gamma}_0 \qquad \gamma^0 = -\frac{\sqrt{A}}{\sin(\chi)}\tilde{\gamma}_0 \qquad \gamma_1 = \frac{1}{\sqrt{A}}\tilde{\gamma}_1$$

$$\gamma^1 = \sqrt{A}\tilde{\gamma}_1 \qquad \gamma_2 = \frac{1}{\sqrt{B}}\tilde{\gamma}_2 \qquad \gamma^2 = \sqrt{B}\tilde{\gamma}_2$$

$$\gamma_3 = \frac{\sin(\theta)}{\sqrt{B}}\tilde{\gamma}_3 \qquad \gamma^3 = \frac{\sqrt{B}}{\sin(\theta)}\tilde{\gamma}_3, \tag{15}$$

where $\tilde{\gamma}_i$, $i = 0, 1, 2, 3$ are the usual Dirac matrices in Minkowski space. The Dirac equation is

$$[\gamma^k(\partial_k - \Gamma_k) - \mu]\Psi = 0, \tag{16}$$

with

$$\Gamma_k = -\tfrac{1}{4}\gamma^j(\partial_k\gamma_j - \gamma_l\Gamma^l_{jk}) + ieA_k. \qquad (17)$$

One finds the following nonvanishing Christoffel symbols $\Gamma^0_{01} = \cot(\chi)$, $\Gamma^1_{00} = \sin(\chi)\cos(\chi)$, $\Gamma^2_{33} = -\sin(\theta)\cos(\theta)$, and $\Gamma^3_{23} = \cot(\theta)$. Then, due to our choice for A_i, we get $\Gamma_0 = -\tfrac{1}{2}\cos(\chi)\tilde\gamma_0\tilde\gamma_1 + ieA_0$, $\Gamma_1 = 0$, $\Gamma_2 = 0$, and $\Gamma_3 = \tfrac{1}{2}\cos(\theta)\tilde\gamma_2\tilde\gamma_3$. Then the Dirac equation becomes

$$\left[-\frac{\sqrt{A}}{\sin(\chi)}\tilde\gamma_0(\partial_\psi - ieA_0) + \sqrt{A}\tilde\gamma_1\left(\partial_\chi + \frac{1}{2}\cot(\chi)\right)\right.$$
$$\left. + \sqrt{B}\left(\tilde\gamma_2\left(\partial_\theta + \frac{1}{2}\cot(\theta)\right) + \tilde\gamma_3\frac{1}{\sin(\theta)}\partial_\phi\right) - \mu\right]\Psi = 0.$$
$$(18)$$

By posing $\Psi = (\sin(\chi))^{-1/2}(\sin(\theta))^{-1/2}\zeta$, we eliminate the terms proportional to $\cot(\theta)$ and to $\cot(\chi)$ in the previous equation. We now consider a static solution with $\zeta = \exp(-i\omega\psi)\eta(\chi,\theta,\phi)$. Then a trivial manipulation of the Dirac equation leads to the following eigenvalue equation:

$$H\eta = \omega\eta, \qquad (19)$$

with

$$H = -i\tilde\gamma_0\tilde\gamma_1\sin(\chi)\partial_\chi - eA_0\mathbb{I}_4 + \sqrt{\frac{B}{A}}\sin(\chi)\tilde\gamma_1 K$$
$$+ i\tilde\gamma_0\frac{\mu}{\sqrt{A}}\sin(\chi). \qquad (20)$$

$\mathbb{I}_4$ stays for the 4×4 identity matrix and K is the following operator:

$$K = -i\tilde\gamma_1\tilde\gamma_0\tilde\gamma_2\partial_\theta - i\tilde\gamma_1\tilde\gamma_0\tilde\gamma_3\frac{1}{\sin(\theta)}\partial_\phi \qquad (21)$$

which commutes with H and whose eigenvalues are $k \in \mathbb{Z} - 0$ [23,24]. By restricting H to eigenspaces of K and by choosing

$$\tilde\gamma_0 = \begin{pmatrix} i\mathbb{I}_2 & \mathbb{O}_2 \\ \mathbb{O}_2 & -i\mathbb{I}_2 \end{pmatrix}, \qquad \tilde\gamma_1 = \begin{pmatrix} \mathbb{O}_2 & \mathbb{I}_2 \\ \mathbb{I}_2 & \mathbb{O}_2 \end{pmatrix}$$

($\mathbb{I}_2$ is the 2×2 identity matrix, $\mathbb{O}_2$ is the 2×2 zero matrix), we obtain the reduced Hamiltonian,

$$H_k = -\sin(\chi)\partial_\chi\begin{pmatrix} \mathbb{O}_2 & -\mathbb{I}_2 \\ \mathbb{I}_2 & \mathbb{O}_2 \end{pmatrix} + eQ\frac{B}{A}\cos(\chi)\begin{pmatrix} \mathbb{I}_2 & \mathbb{O}_2 \\ \mathbb{O}_2 & \mathbb{I}_2 \end{pmatrix}$$
$$+ \sqrt{\frac{B}{A}}\sin(\chi)k\begin{pmatrix} \mathbb{O}_2 & \mathbb{I}_2 \\ \mathbb{I}_2 & \mathbb{O}_2 \end{pmatrix}$$
$$- \frac{\mu}{\sqrt{A}}\sin(\chi)\begin{pmatrix} \mathbb{I}_2 & \mathbb{O}_2 \\ \mathbb{O}_2 & -\mathbb{I}_2 \end{pmatrix}$$
$$= h_k \otimes \mathbb{I}_2, \qquad (22)$$

where

$$h_k = \begin{bmatrix} eQ\frac{B}{A}\cos(\chi) - \frac{\mu}{\sqrt{A}}\sin(\chi) & \sin(\chi)\partial_\chi + \sqrt{\frac{B}{A}}\sin(\chi)k \\ -\sin(\chi)\partial_\chi + \sqrt{\frac{B}{A}}\sin(\chi)k & eQ\frac{B}{A}\cos(\chi) + \frac{\mu}{\sqrt{A}}\sin(\chi) \end{bmatrix}.$$
$$(23)$$

The coordinate transformation

$$x = \log\left(\tan\left(\frac{\chi}{2}\right)\right) \leftrightarrow \chi = 2\arctan(\exp(x)) \qquad (24)$$

is such that $x \in \mathbb{R}$ and, furthermore, h_k becomes

$$h_k = \begin{bmatrix} 0 & \partial_x \\ -\partial_x & 0 \end{bmatrix} + P(\chi(x)), \qquad (25)$$

where

$$P(\chi) = \begin{bmatrix} eQ\frac{B}{A}\cos(\chi) - \frac{\mu}{\sqrt{A}}\sin(\chi) & \sqrt{\frac{B}{A}}\sin(\chi)k \\ \sqrt{\frac{B}{A}}\sin(\chi)k & eQ\frac{B}{A}\cos(\chi) + \frac{\mu}{\sqrt{A}}\sin(\chi) \end{bmatrix}.$$
$$(26)$$

h_k is formally self-adjoint in $L^2[\mathbb{R}, dx]^2$ and it is essentially self-adjoint in $C_0^\infty(\mathbb{R})^2$, as follows from corollary to theorem 6.8 (page 99) of [27] (the limit point case occurs both at $x = -\infty$ and at $x = \infty$). It is easy to show that the essential spectrum of h_k coincides with $\mathbb{R}$ and the same is true for the absolutely continuous spectrum. The latter claim can be checked by following the ideas displayed in Sec. III B. See Appendix A for more details.

V. ULTRACOLD CASE

There is still a subcase to be taken into account. It corresponds to the so-called ultracold case [32], where the three horizons coincide: $r_- = r_+ = r_c$. Also in this case the metric (1) is no more valid, and a suitable limit has to be considered [32]. Actually, one can introduce two different metrics for the ultracold case. As a consequence, also our analysis is split into two parts.

A. Ultracold I

A first metric [32] is

$$ds^2 = -\chi^2 d\psi^2 + d\chi^2 + \frac{1}{2\Lambda}(d\theta^2 + \sin^2(\theta)d\phi^2), \quad (27)$$

with $\chi \in (0, \infty)$ and $\psi \in \mathbb{R}$. One gets $\Gamma^0_{01} = \frac{1}{\chi}$, $\Gamma^1_{00} = \chi$, $\Gamma^2_{33} = -\sin(\theta)\cos(\theta)$, and $\Gamma^3_{23} = \cot(\theta)$. The electromagnetic field strength is $F = \sqrt{\Lambda}\chi d\chi \wedge d\psi$, and we can choose $A_0 = \frac{\sqrt{\Lambda}}{2}\chi^2$ and $A_j = 0$, $j = 1, 2, 3$. We introduce

$$\gamma_0 = \chi \tilde{\gamma}_0 \qquad \gamma^0 = -\frac{1}{\chi} \tilde{\gamma}_0$$

$$\gamma_1 = \tilde{\gamma}_1 \qquad \gamma^1 = \tilde{\gamma}_1$$

$$\gamma_2 = \frac{1}{\sqrt{2\Lambda}} \tilde{\gamma}_2 \qquad \gamma^2 = \sqrt{2\Lambda} \tilde{\gamma}_2$$

$$\gamma_3 = \frac{\sin(\theta)}{\sqrt{2\Lambda}} \tilde{\gamma}_3 \qquad \gamma^3 = \frac{\sqrt{2\Lambda}}{\sin(\theta)} \tilde{\gamma}_3, \qquad (28)$$

and then we obtain $\Gamma_0 = -\frac{1}{2} \tilde{\gamma}_0 \tilde{\gamma}_1 + ieA_0$, $\Gamma_1 = 0$, $\Gamma_2 = 0$, and $\Gamma_3 = \frac{1}{2} \cos(\theta) \tilde{\gamma}_2 \tilde{\gamma}_3$. Calculations which are strictly analogous to the ones performed in the Nariai case [with $\Psi = \exp(-i\omega\psi) \frac{1}{\sqrt{\chi}\sqrt{\sin(\theta)}} \zeta$] and the variable change $\chi = \exp(x)$, $x \in \mathbb{R}$, lead to the following reduced Hamiltonian:

$$h_k = \begin{bmatrix} -\frac{e\sqrt{\Lambda}}{2}\exp(2x) - \mu\exp(x) & \partial_x + \sqrt{2\Lambda}k\exp(x) \\ -\partial_x + \sqrt{2\Lambda}k\exp(x) & -\frac{e\sqrt{\Lambda}}{2}\exp(2x) + \mu\exp(x) \end{bmatrix}. \qquad (29)$$

As in the Nariai case, h_k is formally self-adjoint in $L^2[\mathbb{R}, dx]^2$ and it is essentially self-adjoint in $C_0^\infty(\mathbb{R})^2$, as follows from corollary to theorem 6.8 (page 99) of [27]. The analysis of the spectrum can be pursued by means of the decomposition method applied to the absolutely continuous spectrum, and one can again conclude that the absolutely continuous spectrum of the self-adjoint extension of h_k on $\mathbb{R}$ coincides with the whole real line. See Appendix B for details.

B. Ultracold II

The second allowed metric [32] for the ultracold case is

$$ds^2 = -d\psi^2 + dx^2 + \frac{1}{2\Lambda}(d\theta^2 + \sin^2(\theta)d\phi^2), \qquad (30)$$

with $x \in \mathbb{R}$ and $\psi \in \mathbb{R}$. One gets $\Gamma_{33}^2 = -\sin(\theta)\cos(\theta)$ and $\Gamma_{23}^3 = \cot(\theta)$. The electromagnetic field strength is $F = -\sqrt{\Lambda}d\psi \wedge dx$, and we can choose $A_0 = \sqrt{\Lambda}x$ and $A_j = 0$, $j = 1, 2, 3$. We introduce

$$\gamma_0 = \tilde{\gamma}_0 \qquad \gamma^0 = -\tilde{\gamma}_0$$

$$\gamma_1 = \tilde{\gamma}_1 \qquad \gamma^1 = \tilde{\gamma}_1$$

$$\gamma_2 = \frac{1}{\sqrt{2\Lambda}} \tilde{\gamma}_2 \qquad \gamma^2 = \sqrt{2\Lambda} \tilde{\gamma}_2$$

$$\gamma_3 = \frac{\sin(\theta)}{\sqrt{2\Lambda}} \tilde{\gamma}_3 \qquad \gamma^3 = \frac{\sqrt{2\Lambda}}{\sin(\theta)} \tilde{\gamma}_3, \qquad (31)$$

and then we obtain $\Gamma_0 = ieA_0$, $\Gamma_1 = 0$, $\Gamma_2 = 0$, and $\Gamma_3 = \frac{1}{2} \cos(\theta) \tilde{\gamma}_2 \tilde{\gamma}_3$. Again calculations as above [with $\Psi = \exp(-i\omega\psi) \frac{1}{\sqrt{\sin(\theta)}} \zeta$] lead to the following reduced Hamiltonian:

$$h_k = \begin{bmatrix} -e\sqrt{\Lambda}x - \mu & \partial_x + \sqrt{2\Lambda}k \\ -\partial_x + \sqrt{2\Lambda}k & -e\sqrt{\Lambda}x + \mu \end{bmatrix}. \qquad (32)$$

Also in this case, h_k is formally self-adjoint in $L^2[\mathbb{R}, dx]^2$ and it is essentially self-adjoint in $C_0^\infty(\mathbb{R})^2$. As in the previous case, the decomposition method applied to the absolutely continuous spectrum allows one to draw the conclusion that the spectrum of the self-adjoint extension of the Hamiltonian (32) is absolutely continuous and coincides with $\mathbb{R}$. See Appendix C for details.

VI. PAIR CREATION AND LEVEL CROSSING

We follow the Ruffini-Damour-Deruelle [14–17] approach, which was summarized in a previous paper [18]. Herein, we limit ourselves to recall some very basic properties, focusing on the RN-dS case (the other cases can be dealt with analogously). In this approach one introduces effective potentials $E_0^\pm(r)$ for the positive and negative energy states, respectively; they represent the classical turning points for the particle motion and lead to the definition of the so-called effective ergosphere. These potentials enter the Hamilton-Jacobi (HJ) equation for a classical particle. They can be interpreted also at the quantum level, as in [17]. In particular, they indicate the regions of level crossing between positive and negative energy states [15,16]. In the case of the Dirac equation, it is known that the HJ equation corresponds to a WKB approximation to the Dirac equation at the lowest order [34,35]. Variable separation in the quantum case allows one to obtain an obvious improvement of the semiclassical formulas, amounting to replacing the classical value of the angular momentum with the quantum eigenvalues of the corresponding quantum operator [18]. We limit ourselves to recall one of the main points of our analysis of the Dirac Hamiltonian in [18]. The key observation resides in the following fact: if one considers the potential term in the Dirac Hamiltonian,

$$V(r) = \begin{bmatrix} p_{11}(r) & p_{12}(r) \\ p_{21}(r) & p_{22}(r) \end{bmatrix},$$

and formally calculates the eigenvalues of the above matrix, which are found by solving

$$(p_{11}(r) - \lambda)(p_{22}(r) - \lambda) - p_{12}(r)p_{21}(r) = 0, \qquad (33)$$

then, defining $S(r) \equiv \sqrt{(p_{11}(r) + p_{22}(r))^2 - 4p_{11}(r)p_{22}(r) + 4p_{12}(r)p_{21}(r)}$ one finds

$$\lambda^\pm(r) = \frac{1}{2}(p_{11}(r) + p_{22}(r) \pm S(r)), \qquad (34)$$

and moreover one gets

$$\lambda^\pm(r) = E_0^\pm(r), \qquad (35)$$

i.e., the semiclassical potentials introduced by Damour-Deruelle-Ruffini coincide with the eigenvalues of the matrix potential term in the Dirac Hamiltonian. Moreover, the

square of the classical angular momentum term is replaced by the square of the eigenvalues $k = \pm(j + 1/2)$ for the quantum angular momentum, and one obtains

$$E_0^\pm(r) = \frac{eQ}{r} \pm \sqrt{f(r)\left(\mu^2 + \frac{k^2}{r^2}\right)}. \tag{36}$$

A. Level crossing in the RN-dS case

Level crossing amounts to the presence of overlap between the range of E_0^+ and the range of E_0^-, signalling the possibility of a tunneling between positive energy states and negative energy ones; the latter phenomenon is in turn interpreted as pair creation at the barrier potential, and is strictly related to the Klein paradox (incidentally, it could be called for this reason also Klein effect [29]). There is a peculiar property in the case of RN-dS black holes: due to the inequality $\Phi_c \neq \Phi_+$, an overlap is always present, indeed one gets

$$\lim_{r \to r_+} E_0^\pm(r) = \Phi_+, \tag{37}$$

and

$$\lim_{r \to r_c} E_0^\pm(r) = \Phi_c. \tag{38}$$

Assuming for definiteness $eQ > 0$, one finds

$$E_0^-(r_+) = \Phi_+ > \Phi_c = E_0^+(r_c), \tag{39}$$

which proves the above claim. Moreover, it is easy to realize that level crossing occurs for energy ω such that

$$\Phi_c = \min E_0^+(r) \le \omega \le \max E_0^-(r) = \Phi_+. \tag{40}$$

For $eQ < 0$ the overlap still exists, being $E_0^-(r_c) = \Phi_c > \Phi_+ = E_0^+(r_+)$, and (40) changes accordingly: $\Phi_+ \le \omega \le \Phi_c$. It is to be immediately pointed out that this overlap is not enough to conclude that a sensible pair-creation process occurs in the given background. Indeed, the potential barrier to be overcome by the negative energy particle can be as large as the whole external region of the space-time. As a consequence, no efficient process can be expected on this ground in general, and further conditions taking into account the effective largeness of the barrier have to be looked for. Notice also that E_0^+, as a function of μ^2, is increasing, and the same is true for its dependence on k^2; both these properties are reversed in the case of E_0^-, which is in fact decreasing. As a consequence, one expects a more difficult level crossing for increasing values of μ^2 or k^2.

We start giving sample examples for a nonextremal black hole manifold. In Fig. 1, we keep fixed the geometric background parameters L, M, Q, and the charge e of the Dirac particle, and consider two sample values of the mass. On the left, we find the former phenomenon described above, i.e. a level crossing with a barrier as large as $\sim r_c - r_+$. On the right-hand case, which is obtained by considering a lower fermion mass, we obtain instead a level crossing associated with a much smaller extent of the barrier. The latter case is expected to be involved in an effective phenomenon of pair creation at the barrier. In Figs. 2 and 3 a further nonextremal case is displayed, with $\frac{r_c}{r_+} \sim 1.01$ (to be compared with $\frac{r_c}{r_+} \sim 10.4$ of the example
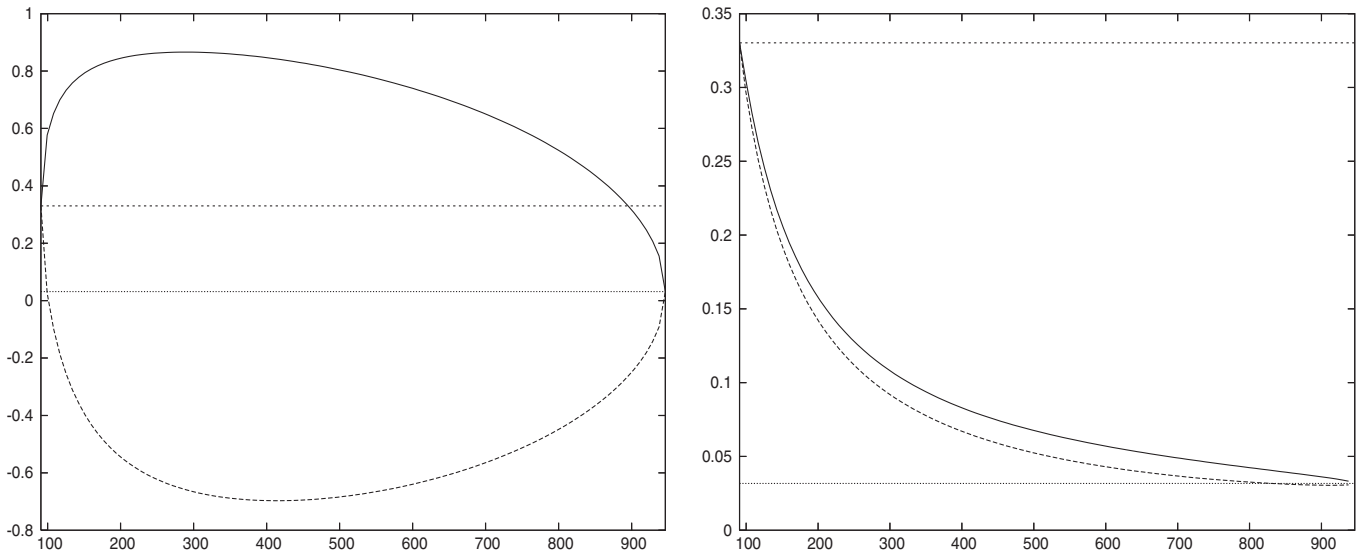

FIG. 1.   On the left, we display the level crossing in the case of a nonextremal RN-dS black hole, with $L = 1000$, $M = 50$, $Q = 30$, $\mu = 1$, $e = 1$, and $k = 1$. The particle and the black hole have charges with the same sign. One finds $r_+ \sim 90.842$, $r_c \sim 946.214$, $r_- \sim 9.999$, and $r_0 \sim -1047.056$. The upper straight line represents eQ/r_+, the lower is eQ/r_c. The upper potential is $E_0^+(r)$, the lower one is $E_0^-(r)$. Level crossing occurs, but the potential barrier is as large as the whole space-time region at hand. On the right, the only change with respect to the previous figure stays in the smaller value $\mu = 0.01$ of the fermion mass. The upper straight line represents eQ/r_+, the lower is eQ/r_c. The upper potential is $E_0^+(r)$, the lower one is $E_0^-(r)$. Level crossing occurs in this case with a much smaller extent of the potential barrier with respect to $r_c - r_+$.
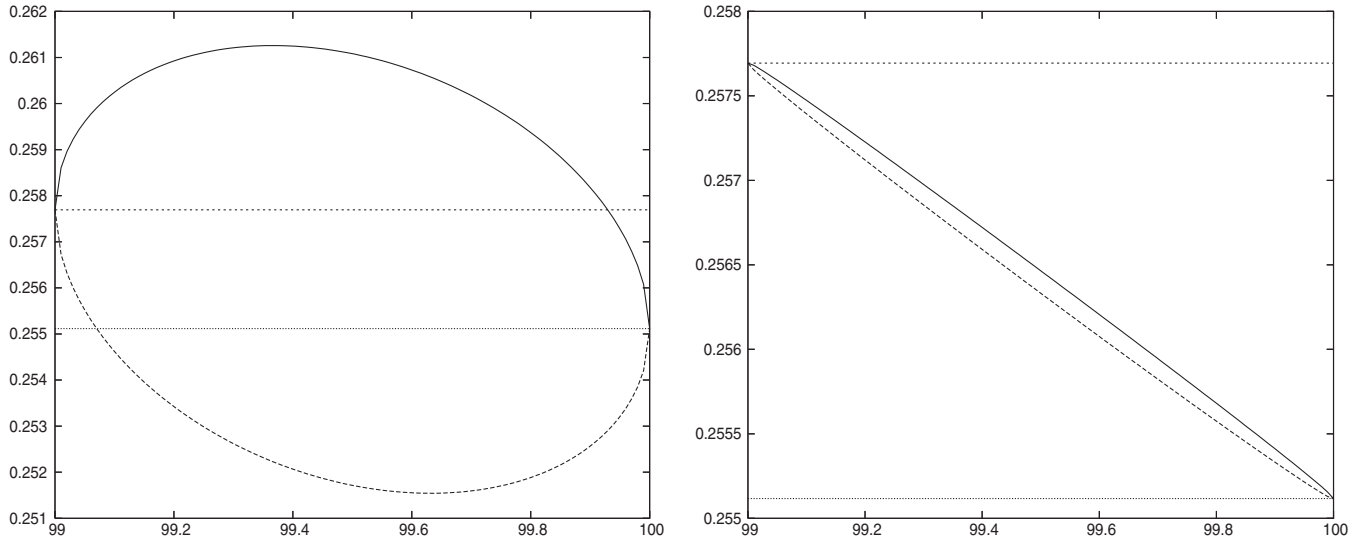
FIG. 2. Level crossing in the case of a nonextremal RN-dS black hole having $L = \sqrt{31\,791}$, $M = 1\,193\,005/31\,791$, and $Q = 330\sqrt{190}/\sqrt{31\,791}$, which are such that $r_c = 100$, $r_+ = 99$, and $r_- = 10$. Moreover, we choose $e = 1$, $k = 1$, and the same sign for the black hole charge and for the particle charge. The upper straight line represents eQ/r_+, the lower is eQ/r_c. The figure on the right displays the potentials for $\mu = 1$, and shows that a very large potential barrier occurs. In the figure on the right, one has $\mu = 0.01$ and a very narrower potential barrier. Note that in the latter case $eQ/r_+ > \mu$ holds, whereas in the former the opposite inequality is implemented.

displayed in Fig. 1). In Fig. 3 we show the details of the potentials near the horizons. In Fig. 4, an extremal case is also shown. In Fig. 5 we display the so-called lukewarm case [32,36], which is such that the same temperature occurs in the case of the cosmological horizon and of the black hole event horizon, still with $r_+ < r_c$ (this happens for $Q = M$). It is displayed for the sake of completeness, even if from the point of view of the given phenomenon no peculiar behavior is expected with respect to the cases

explored in Figs. 1 and 2. Notice that, from a physical point of view, the phenomenon of pair creation by a charged black hole has been related to the Schwinger calculation of pair creation by a homogeneous electric field [7]. The highest value of the electrostatic potential, which corresponds to the highest intensity of the electrostatic field, occurs near the black hole event horizon; hence, one could naively expect that the standard condition $\Phi_+^2 > \mu^2$, i.e.
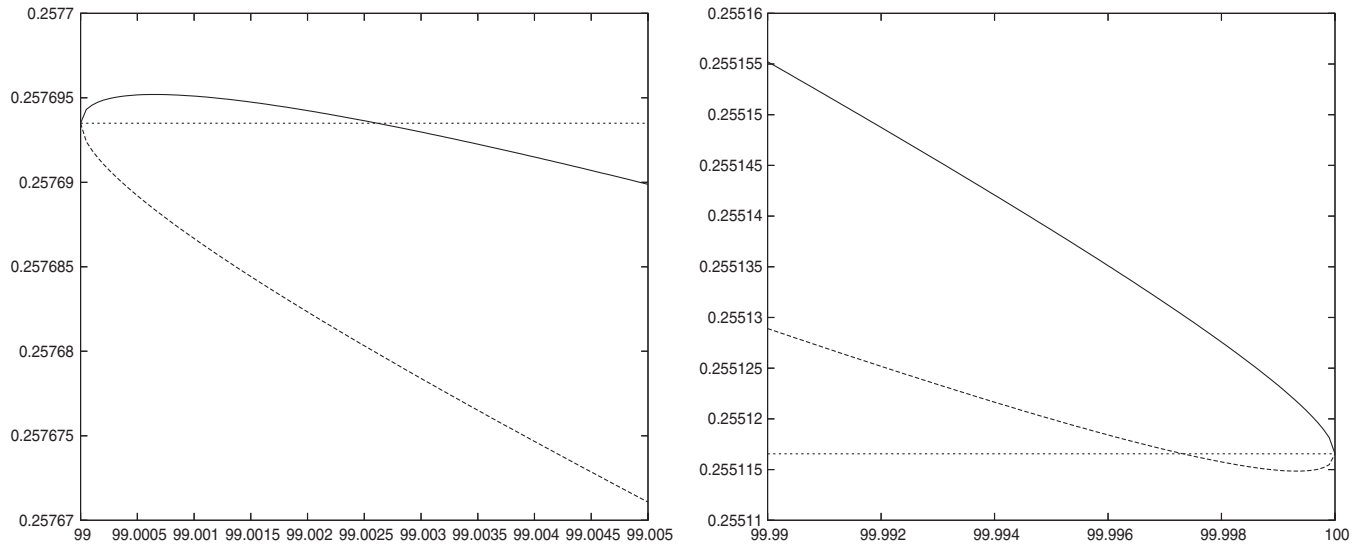

FIG. 3. Level crossing in the case of a nonextremal RN-dS black hole having $L = \sqrt{31\,791}$, $M = 1\,193\,005/31\,791$, and $Q = 330\sqrt{190}/\sqrt{31\,791}$, as in the previous figure, with $e = 1$, $k = 1$. We display on the left the presence of a bump near the black hole horizon in the case of E_0^+. Analogously, on the right we show the behavior of the potentials very near the cosmological horizon.
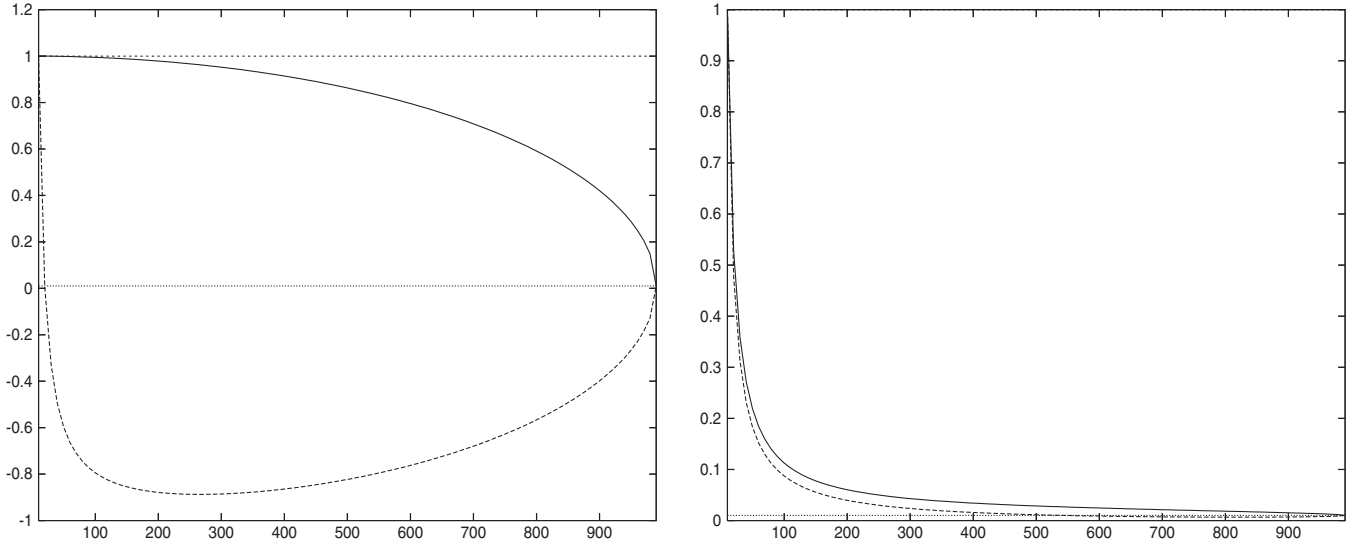
FIG. 4. Level crossing in the case of an extremal RN-dS black hole, with $L = 1000$, $Q = 10$ and then $M \simeq 9.999\,499$ [see Eq. (5)]. Particle parameters $e = 1$, $k = 1$ are kept fixed, whereas it holds $\mu = 1$ on the left and $\mu = 0.01$ on the right. Level crossing is more effective in the latter case, and it occurs without any bump near the black hole event horizon.

$$\left(\frac{Q}{r_+}\right)^2 > \frac{\mu^2}{e^2}, \qquad (41)$$

which is enough for the standard Reissner-Nordström case [7,8,15], is also qualitatively relevant in the present one, at least in some approximation. We recall that, in the case of the lightest known charged particle, i.e. the electron, one has $\frac{\mu_e}{e} \sim 10^{-21}$. The above condition is not necessary for the existence of a sensible level crossing. A proof of its sufficiency in the extremal case can be given under the hypothesis $\frac{k^2}{r_+^2} \ll 1$, which allows one to neglect the angular

momentum contribution in the potentials, and also for $r_+ \ll r_c$. In the extremal case, it is easy to show that the condition to be satisfied is that $\frac{dE_0^+}{dr}(r_+)\frac{dE_0^-}{dr}(r_+) > 0$, which means that both potentials are increasing or decreasing near $r = r_+$. One has to impose

$$\frac{dE_0^+}{dr}(r_+)\frac{dE_0^-}{dr}(r_+) = \frac{1}{r_+^2}\left[\Phi_+^2 - \frac{r_c^2}{L^2}\left(1 - \frac{r_+}{r_c}\right)\left(1 + 3\frac{r_+}{r_c}\right)\right.$$
$$\left. \times \left(\mu^2 + \frac{k^2}{r_+^2}\right)\right] > 0, \qquad (42)$$
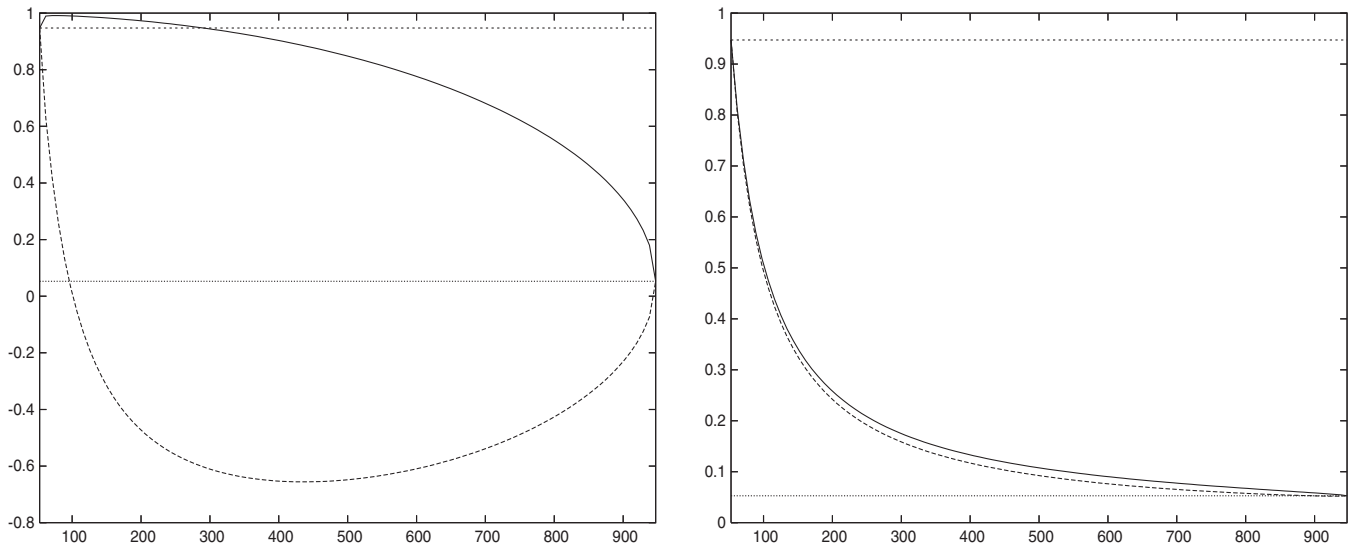

FIG. 5. Level crossing in the case of a lukewarm RN-dS black hole, with $L = 1000$, $M = 50$, $Q = 50$, $e = 1$, $k = 1$, and with $\mu = 1$ on the left and $\mu = 0.01$ on the right. One finds $r_+ \sim 52.786$ and $r_c \sim 947.214$. Level crossing is qualitatively similar to the one displayed in Fig. 1.
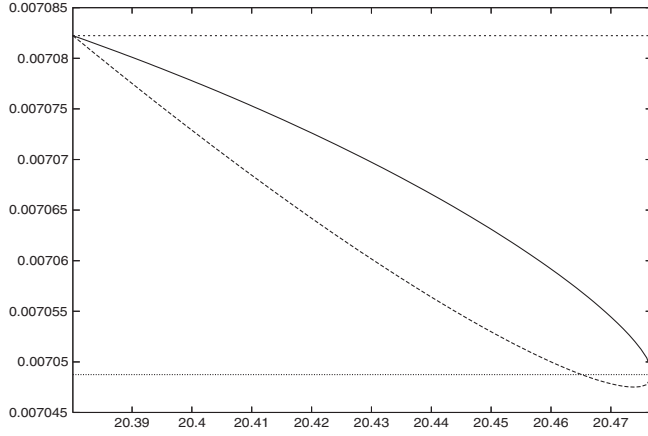
FIG. 6. Level crossing in the case of an extremal RN-dS black hole, with $L = 50$, $Q = 14.433\,684\,560\,776\,572\,5$, which are such that $M = 13.608\,225\,263\,871\,805\,121$, $r_+ \simeq 20.380\,115$, and $r_c \simeq 20.476\,977$. With $\mu = 0.01$, $e = 0.01$, $k = 1$ one gets $\Phi_+ \simeq 0.708\mu$, which violates (41).

and then, under the above hypotheses $\frac{k^2}{r_+^2} \ll 1$ and $r_+ \ll r_c$, one obtains

$$\frac{dE_0^+}{dr}(r_+)\frac{dE_0^-}{dr}(r_+) \simeq \frac{1}{r_+^2}\left(\Phi_+^2 - \mu^2\frac{r_c^2}{L^2}\right) > 0, \quad (43)$$

for which, being $\frac{r_c}{L} < 1$, the aforementioned condition (41) is sufficient. In Fig. 6 we show an example of extremal black hole where a significant level crossing occurs but condition (41) is not satisfied.

Explicit evaluations of the transmission coefficient which is related to the pair-creation phenomenon (discharge) can be given, e.g. in a WKB approximation, as
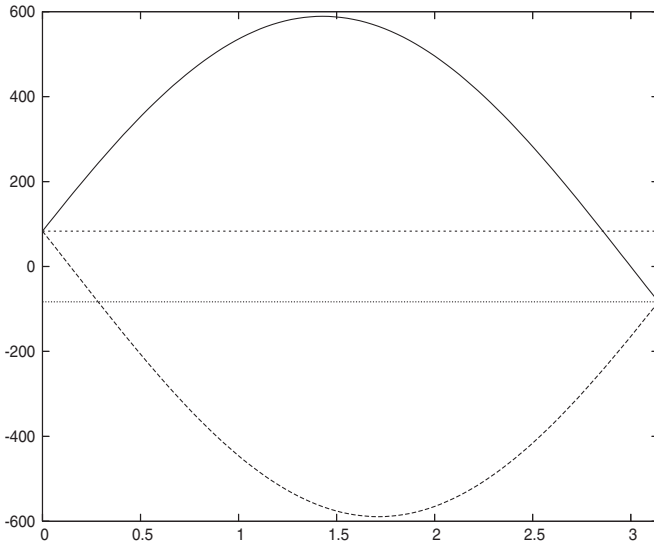
pointed out in the original literature [7,8,15]. See also [18] for a short summary. We do not delve into quantitative evaluation herein in the RN-dS case but limit ourselves to some estimates in the cases which will be analyzed in the following subsections.

B. The Nariai case

The potentials $E_0^\pm(\chi)$ in the Nariai case are

$$E_0^\pm(\chi) = eQ\frac{B}{A}\cos(\chi) \pm \sqrt{\frac{\mu^2}{A} + k^2\frac{B}{A}}\sin(\chi). \quad (44)$$

Also in this case level crossing is always present, being $E_0^+(\pi) < E_0^-(0)$ for $eQ > 0$ and $E_0^+(0) < E_0^-(\pi)$ for $eQ < 0$. Level crossing occurs for energies ω such that $E_0^+(\pi) \leq \omega \leq E_0^-(0)$ in the former case and for $E_0^+(0) \leq \omega \leq E_0^-(\pi)$ in the latter one. Again, the largeness of the potential barrier depends on the choice of the parameters. See Fig. 7.

An estimation of the transmission coefficient can be given in the WKB approximation; one obtains [15]

$$|T_\omega^{\mathrm{WKB}}|^2 = \exp\left(-2\int_{\mathrm{barrier}} dx\sqrt{Z_\omega}\right), \quad (45)$$

where x stays for the coordinate defined in (24) and where we have stressed the dependence on the energy ω of T_ω^{WKB} and of

$$Z_\omega = \left(\frac{B}{A}k^2 + \frac{\mu^2}{A}\right)\sin^2(\chi(x)) - \left(\omega - eQ\frac{B}{A}\cos(\chi(x))\right)^2. \quad (46)$$
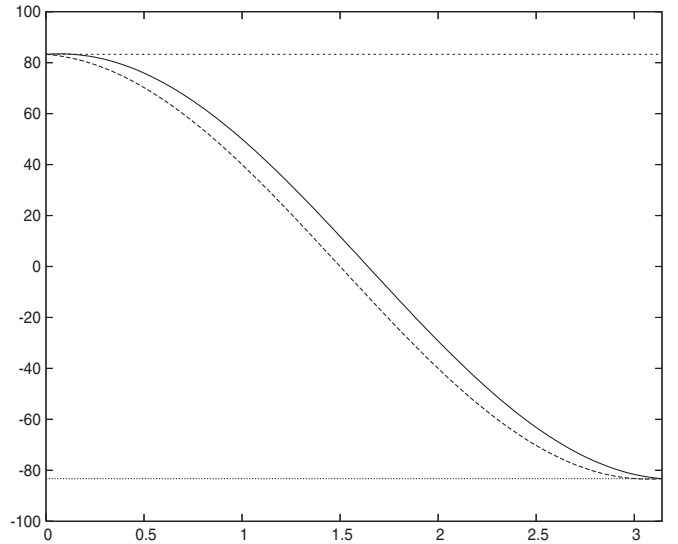
Let us introduce

FIG. 7. Level crossing in the case of a Nariai solution. The potentials $E_0^\pm(\chi)$ are plotted, with $L = 1000$, $Q = 80$. Particle parameters $e = 1$, $k = 1$ are kept fixed; particle mass is chosen to be $\mu = 1$ on the left and $\mu = 0.01$ on the right. Also in the latter case, a bump is present for E_0^+ near $\chi = 0$ and a hollow occurs for E_0^- near $\chi = \pi$.

$$\mu_k^2 = \frac{B}{A}k^2 + \frac{\mu^2}{A}, \qquad (47)$$

and also

$$E_m = |Q|\frac{B}{A}, \qquad (48)$$

which corresponds to $\frac{1}{A}$ times the maximum value for the modulus of the electrostatic field. Note that positivity of Z_ω requires $\omega^2 < \mu_k^2 + e^2 E_m^2$. We obtain

$$|T_\omega^{\mathrm{WKB}}|^2 = \exp\left(-2\pi|e|E_m\left(\sqrt{1 + \frac{\mu_k^2}{e^2 E_m^2}} - 1\right)\right), \quad (49)$$

which does not depend on ω. See Appendix D for more details. At the leading order as $\mu_k^2 \ll e^2 E_m^2$ one is also able to recover the approximation

$$|T_\omega^{\mathrm{WKB}}|^2 \sim \exp\left(-\pi\frac{\mu_k^2}{|e|E_m}\right), \qquad (50)$$

which shares a nice resemblance with the WKB estimate of the transmission coefficient related to the pair-creation process in a uniform constant electrostatic field. Compare e.g. [15].

C. The ultracold cases

We obtain

$$E_{\mathrm{I}}^{\pm}(\chi) = -\frac{e\sqrt{\Lambda}}{2}\chi^2 \pm \sqrt{2\Lambda k^2 + \mu^2}\chi \qquad (51)$$

in the case of the first kind of ultracold solution (27), and level crossing requires that $\omega \leq 0$ for $e > 0$ and $\omega \geq 0$ for $e < 0$. In the case (30) one finds

$$E_{\mathrm{II}}^{\pm}(x) = -e\sqrt{\Lambda}x \pm \sqrt{2\Lambda k^2 + \mu^2}. \qquad (52)$$

It is evident that for any $\omega \in \mathbb{R}$ one obtains level crossing. In Figs. 8 and 9 level crossing is displayed for both the ultracold I and the ultracold II cases.

As to a WKB approximation for $|T_\omega|^2$, we get in both cases

$$|T_\omega^{\mathrm{WKB}}|^2 = \exp\left(-\frac{\pi(\mu^2 + 2\Lambda k^2)}{|e|\sqrt{\Lambda}}\right), \qquad (53)$$

which again is independent from ω. Notice that, by keeping into account that for the electrostatic field one finds $E = \sqrt{\Lambda}$, and with the replacement $\mu^2 \mapsto \mu_k^2 = \mu^2 + 2\Lambda k^2$, one obtains again a formula which is very similar to the one which is associated with the description of the pair creation in a uniform constant electric field in flat space-time in the same approximation, and this time no requirement about the smallness of the ratio between μ_k^2 and $|e|E$ is imposed. A deeper analysis for the special cases ultracold II, ultracold I, and Nariai is in progress [37].

Some considerations about the problem of the choice of the quantum state playing the role of vacuum are addressed. If one were to assume that the positive and negative frequencies associated with the Hamiltonian define the vacuum, one would end up with the so-called Boulware vacuum, which is viable as the real vacuum only in the ultracold II case, where the background temperature is zero [36]. For a Reissner-Nordström-de Sitter black hole background, a further difficulty arises due to the presence of both a cosmological temperature and of a black hole temperature in the nonextremal and nonlukewarm cases, involving a true nonequilibrium situation. A simpler case is the extremal one, because of the occurrence of a single
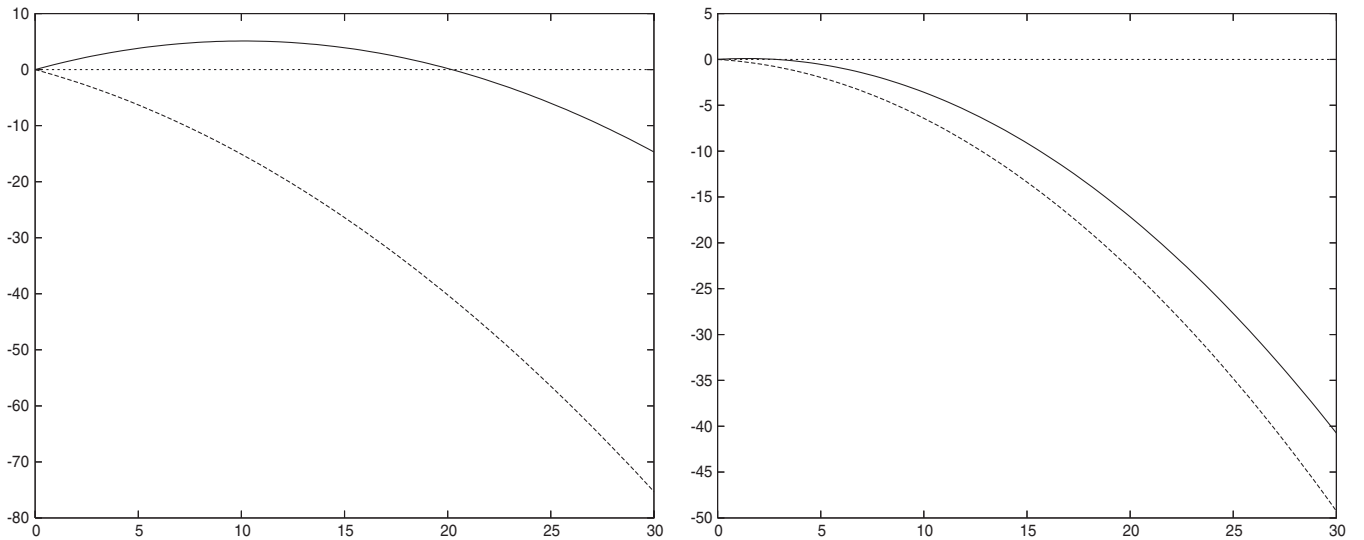

FIG. 8.   Level crossing in the case of the ultracold I metric. We choose $\Lambda = 0.01$, $k = 1$, and $e = 1$ in both cases and $\mu = 1$ on the left and $\mu = 0.01$ on the right. We display only a part of the full plot (but qualitatively all relevant information is given). The potentials converge both to zero as $\chi \to 0$ and to $-\infty$ as $\chi \to +\infty$.
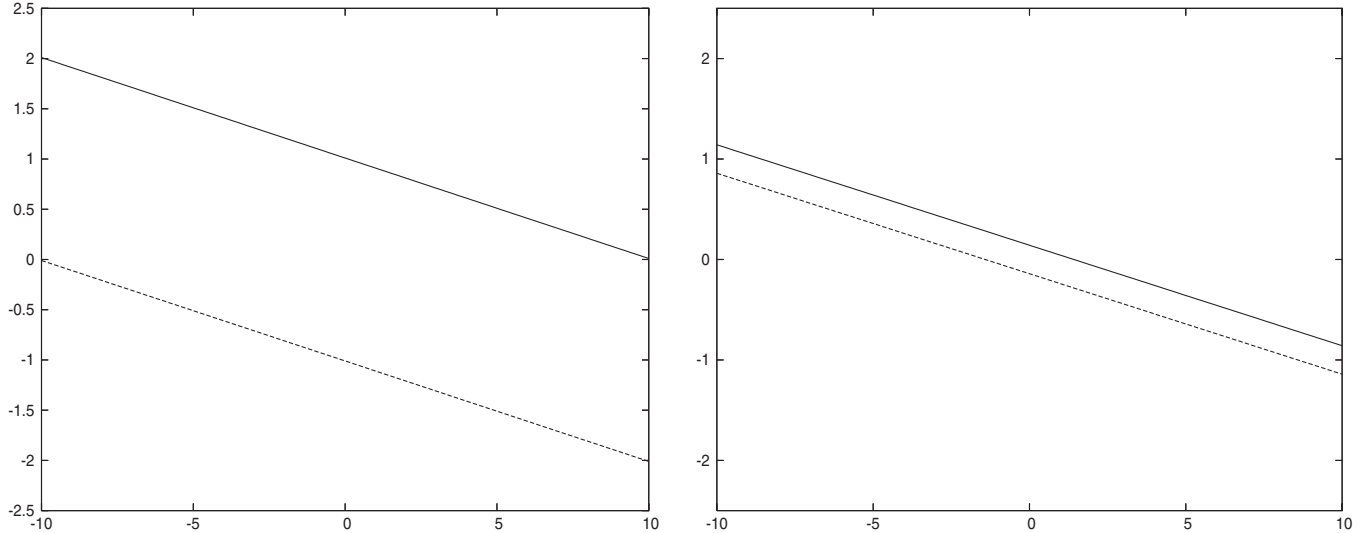
FIG. 9.   Level crossing in the case of the ultracold II metric. We choose $\Lambda = 0.01$, $k = 1$, and $e = 1$ in both cases and $\mu = 1$ on the left and $\mu = 0.01$ on the right. We display only a part of the full plot, which shows of course a linear behavior.

temperature for the given manifold, and the same considerations can be made in the case of the lukewarm solution and in the Nariai case.

We are not aware of a rigorous construction for quantum field theory on the given backgrounds. One could expect that, in the presence of a single nonzero temperature, suitable analyticity requirements for the fields on the extended manifold can lead to the thermal state as in [7], and that "heating up" the Boulware vacuum (as it can be rigorously done in the case of a scalar field on a Schwarzschild black hole background [38]), taking into account the complication of the level crossing displayed above, could be a viable solution. The instability associated with the pair-creation process induced by the presence of the electrostatic field generated by the black hole still remains, and gives rise to the process of discharge we have taken into account. Thermality of the physical state modifies such a pair-creation process but the transmission coefficient $|T|$ we have calculated for a vacuum situation still plays a role, as it is shown e.g. in Ref. [39] for the case of quantum electrodynamics in flat space-time (see also [40]). One obtains that for an initial thermal state pair creation is still proportional to $|T|^2$ with a multiplicative factor depending on the temperature. We shall come back to this topic in [37]. The general RN-dS case is evidently more tricky and challenging, and requires a nonequilibrium framework.

VII. CONCLUSIONS

We have shown that, on the background of a charged black hole in de Sitter space, massive and charged Dirac particles are described by a Hamiltonian operator which is well behaved both on the cosmological horizon and on the black hole horizon. We have also inferred that in all cases the point spectrum of the Hamiltonian is empty, and then there is no bound state and no normalizable time-periodic solution of the Dirac equation. The presence of two different horizons allows a simpler analysis even in the extremal case. Moreover, the same occurrence of two event horizons involving different values of the electrostatic potential is at the root of the presence in any case of level crossing between positive energy states and negative energy ones. This fact *per se* is not enough for claiming that a sensible pair-creation effect is present on the given manifold, due to the fact that *a priori* the potential barrier to be overcome can be very large (even large as almost the whole external manifold in the RN-dS case and in the Nariai one) and then the effect is expected to be very suppressed. Nevertheless, in all cases examples can be found where the barrier is of much more reduced extent, in such a way to allow a physical ground to the pair-creation phenomenon. Some estimates in WKB approximation have been given for the transmission coefficient which is related to the pair-creation process [7,8,15] in the case of the Nariai geometry and in the ultracold ones.

APPENDIX A: ABSOLUTELY CONTINUOUS SPECTRUM IN THE NARIAI CASE

We introduce a decomposition point $\bar{d} \in \mathbb{R}$ and also the following self-adjoint operators $H_{-\infty}$ and H_{∞} on the respective domains $D(H_{-\infty}) = \{\vec{g} \in L^2[(-\infty, \bar{d}], dx]^2,$ $\vec{g}$ is locally absolutely continuous; $g_1(\bar{d}) = 0$;

$H_{-\infty}\vec{g} \in L^2[(-\infty, \bar{d}], dx]^2\}$, and analogously $D(H_\infty) = \{\vec{g} \in L^2[[\bar{d}, \infty), dx]^2, \vec{g}$ is locally absolutely continuous; $g_1(\bar{d}) = 0$; $H_\infty\vec{g} \in L^2[[\bar{d}, \infty), dx]^2\}$. We define $P_- := \lim_{x\to-\infty}P(\chi(x))$ and $P_+ := \lim_{x\to-\infty}P(\chi(x))$, where the $P(\chi(x))$ is the potential (26), and write

$$P = P_\mp + (P - P_\mp). \tag{A1}$$

The first term on the right-hand side of Eq. (A1) is obviously of bounded variation, whereas the latter term is such that $|P - P_+| \in L^1[[\bar{d}, \infty), dx]$ and $|P - P_-| \in L^1[(-\infty, \bar{d}], dx]$, respectively. Moreover, notice that

$$P_\mp = \begin{bmatrix} \pm eQ\frac{B}{A} & 0 \\ 0 & \pm eQ\frac{B}{A} \end{bmatrix}. \tag{A2}$$

As a consequence, in both cases the hypotheses of theorem 16.7 in [27] are implemented, and one is allowed to conclude that $H_{-\infty}$ has absolutely continuous spectrum in $\mathbb{R} - \{eQ\frac{B}{A}\}$, and that H_∞ has absolutely continuous spectrum in $\mathbb{R} - \{-eQ\frac{B}{A}\}$. Then the absolutely continuous spectrum of the self-adjoint extension of the Hamiltonian operator (25) is $\mathbb{R}$.

APPENDIX B: ABSOLUTELY CONTINUOUS SPECTRUM IN THE ULTRACOLD I CASE

Let us introduce a self-adjoint extension $H_{-\infty}$ of the formal differential expression (29) on the interval $(-\infty, 0]$ (0 is the decomposition point). Notice that the potential term in (29) is

$$P(x) = \begin{bmatrix} -\frac{e\sqrt{\Lambda}}{2}\exp(2x) - \mu\exp(x) & \sqrt{2\Lambda}k\exp(x) \\ \sqrt{2\Lambda}k\exp(x) & -\frac{e\sqrt{\Lambda}}{2}\exp(2x) + \mu\exp(x) \end{bmatrix} \tag{B1}$$

and it is such that $\lim_{x\to-\infty}P(x) = \mathbb{O}$. Moreover, it is easy to show that $|P(x)| \in L^1[(-\infty, 0], dx]$. As a consequence, theorem 16.7 of [27] can be applied and the given self-adjoint extension has absolutely continuous spectrum in $\mathbb{R} - \{0\}$. It is also true that 0 is not an eigenvalue for $H_{-\infty}$, because no normalizable solution exists as a consequence of the Levinson theorem [whose applicability is related to the property that each entry in $P(x)$ is integrable near $x = -\infty$; cf. [41], page 8]. Compare also [4] for the Kerr-Newman case. Thus $\sigma_{ac}(H_{-\infty}) = \mathbb{R}$. As a consequence (cf. e.g. [22]), also the absolutely continuous spectrum of the self-adjoint extension of h_k on $\mathbb{R}$ coincides with the whole real line.

APPENDIX C: ABSOLUTELY CONTINUOUS SPECTRUM IN THE ULTRACOLD II CASE

Let us notice that the equation $h_k\vec{g} = \lambda\vec{g}$, by putting

$$\vec{g}(x) = \begin{pmatrix} w_1(x)u_1(x) \\ \frac{1}{w_1(x)}u_2(x) \end{pmatrix},$$

where $w_1(x) = \exp(-2\sqrt{2\Lambda}kx)$ is equivalent to the following equation:

$$\frac{d}{dx}\vec{u}(x) = \begin{bmatrix} 0 & (-e\sqrt{\Lambda}x - \alpha)w_1(x) \\ (e\sqrt{\Lambda}x + \beta)\frac{1}{w_1(x)} & 0 \end{bmatrix}\vec{u}(x), \tag{C1}$$

where $\alpha = \lambda - \mu$ and $\beta = \lambda + \mu$. Then, by restricting our attention to the interval $[c, \infty)$, with $c > 0$, and by applying theorem 2 in [31] the result follows. Let us define,

according to the notations of [31], $p_1 = (-e\sqrt{\Lambda}x + \mu)\times\exp(-2\sqrt{2\Lambda}kx) =: p_{11} + p_{12}$, $p_2 = (-e\sqrt{\Lambda}x - \mu)\times\exp(2\sqrt{2\Lambda}kx) =: p_{21} + p_{22}$, $\alpha_1 = \exp(-2\sqrt{2\Lambda}kx)$, and $\alpha_2 = \exp(2\sqrt{2\Lambda}kx)$; $p_{11} := -e\sqrt{\Lambda}x\exp(-2\sqrt{2\Lambda}kx)$ and $p_{21} := -e\sqrt{\Lambda}x\exp(2\sqrt{2\Lambda}kx)$. One obtains $p_{11}p_{21} = e^2\Lambda x^2 > 0$ and $\int_c^{+\infty}dx\sqrt{p_{11}p_{21}} = +\infty$. Moreover, both $\int_c^{+\infty}dx\alpha_1\sqrt{\frac{p_{21}}{p_{11}}}$ and $\int_c^{+\infty}dx\alpha_2\sqrt{\frac{p_{11}}{p_{21}}}$ diverge (it is sufficient that one of them diverges [31]). Moreover, if $\eta = (\frac{p_{21}}{p_{11}})^{1/4}$, then $\Delta := \frac{d\eta}{dx}\frac{1}{\eta\sqrt{p_{11}p_{21}}} = \frac{\sqrt{2\Lambda}|k|}{|e|x}$ is such that $\lim_{x\to+\infty}\Delta = 0$ and $\frac{d\Delta}{dx} \in L^1[[c, +\infty), dx]$. Moreover, $\frac{\alpha_1}{p_{11}}, \frac{\alpha_2}{p_{21}}, \frac{p_{12}}{p_{11}}$, and $\frac{p_{22}}{p_{21}}$ are long range (in the sense that they vanish as $x \to +\infty$ and their derivative is in $L^1[[c, +\infty), dx]$). Then the hypotheses of theorem 2 in [31] are implemented, which means that the absolutely continuous spectrum is $\mathbb{R}$.

APPENDIX D: EVALUATION OF THE NARIAI TRANSMISSION INTEGRAL

We need to evaluate

$$\int_{\text{barrier}}\sqrt{Z_\omega}dx, \tag{D1}$$

where Z_ω is given in (46) and $\chi(x) = 2\arctan e^x$ [cf. (24)]. Using

$$\cos\chi(x) = -\tanh x, \qquad \sin\chi(x) = \frac{1}{\cosh x},$$

we can rewrite

$$\int_{\text{barrier}} \sqrt{Z_\omega} dx = \int_{\text{barrier}} \sqrt{\left(\frac{B}{A}k^2 + \frac{\mu^2}{A}\right) - \left(\omega \cosh x + eQ\frac{B}{A}\sinh x\right)^2} \frac{dx}{\cosh x}$$

$$= \int_{\text{barrier}} \sqrt{\left(\frac{B}{A}k^2 + \frac{\mu^2}{A}\right)e^{-2x} - \frac{1}{4}\left(\left[\omega + eQ\frac{B}{A}\right] + \left[\omega - eQ\frac{B}{A}\right]e^{-2x}\right)^2} \frac{2e^{2x}}{1 + e^{2x}} dx. \qquad \text{(D2)}$$

If we define μ_k^2 as in (47) and $\omega_\pm = \omega \pm eQ\frac{B}{A}$, and change the variable to $z = e^{2x}$ we get

$$\int_{\text{barrier}} \sqrt{Z_\omega} dx = \int_{z_-}^{z_+} dz \frac{1}{1+z} \sqrt{-\frac{\omega_-^2}{4}\frac{1}{z^2} + \left(\mu_k^2 - \frac{1}{2}\omega_+\omega_-\right)\frac{1}{z} - \frac{\omega_+^2}{4}}, \qquad \text{(D3)}$$

where $0 \le z_- < z_+$ are the two real solutions of

$$-\frac{\omega_-^2}{4} + \left(\mu_k^2 - \frac{1}{2}\omega_+\omega_-\right)z - \frac{\omega_+^2}{4}z^2 = 0.$$

Note that such solutions exist if the discriminant of the polynomial is positive. This gives

$$0 < \mu_k^2(\mu_k^2 - \omega_+\omega_-) = \mu_k^2 + e^2Q^2\frac{B^2}{A^2} - \omega^2.$$

The integral is indeed well defined for $-\sqrt{\mu_k^2 + e^2Q^2\frac{B^2}{A^2}} < \omega < \sqrt{\mu_k^2 + e^2Q^2\frac{B^2}{A^2}}$. Note, however, that only the region of level crossing $-|eQB/A| \le \omega \le |eQB/A|$, corresponding to $\omega_+\omega_- \le 0$, is relevant for computing the transmission coefficient. Let us first distinguish the "generic case" $\omega_+\omega_- \ne 0$ from the "particular case" $\omega_+\omega_- = 0$. In order to compute the integral in the generic case, the residue method is used. Let us cut the complex plane $\mathbb{C}$ along the segment $[z_-, z_+] \subset \mathbb{R}_+$ (note that $z_- > 0$ in this case), so defining a Riemann sheet for the square root $f(z) = \sqrt{(z_+ - z)(z - z_-)\omega_+^2/4}$. In particular, we choose the phase of $(z_+ - z)(z - z_-)\omega_+^2/4$ to be 0 (modulo 4π) along the lower border of the cut, so that it will be 2π (modulo 4π) along the upper border. Thus, it makes sense to take the closed path $\Gamma = s_\downarrow \cup c_+ \cup s_\uparrow \cup c_-$ as in Fig. 10.

When the radii of the two circles $c_\pm$ are set to zero, Γ approaches the cut without crossing any singularity so that the value of the integral

$$I = \oint_\Gamma dz \frac{1}{1+z}\frac{f(z)}{z} \qquad \text{(D4)}$$

does not change. In this limit, the contributions from the circles vanish, whereas

$$\int_{s_\downarrow} \to \int_{z_-}^{z^+}, \qquad \int_{s_\uparrow} \to -\int_{z_-}^{z^+}$$
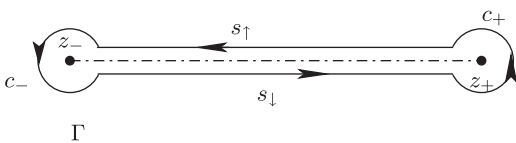

FIG. 10. Circuit Γ around the cut in the Riemann sheet of f.

and being the phase of f equal to 0 on the lower cut and to π on the upper cut, we see that

$$\int_{\text{barrier}} \sqrt{Z_\omega} dx = \int_{z_-}^{z^+} dz \frac{1}{1+z}\frac{f(z)}{z} = \frac{1}{2}I. \qquad \text{(D5)}$$

To compute the integral I, let us blow up Γ, without crossing the poles of the integrand (which are $z = 0, -1, \infty$) as in Fig. 11.

We see that (cf. Fig. 11)

$$I = -\oint_{c_\epsilon(0)} dz \frac{1}{1+z}\frac{f(z)}{z} - \oint_{c_\epsilon(-1)} dz \frac{1}{1+z}\frac{f(z)}{z}$$
$$+ \oint_{c_R(0)} dz \frac{1}{1+z}\frac{f(z)}{z}, \qquad \text{(D6)}$$

where we used $c_r(z)$ to indicate the counterclockwise oriented circle with center z and radius r. Note that, if we take the change of variable $z = 1/t$ in the last integral, we have [42] $c_R(0) \to -c_{1/R}(0)$ so that

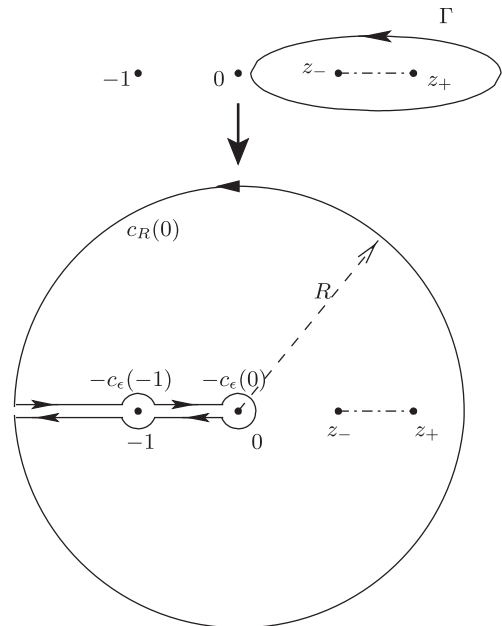FIG. 11. Blowup of the path Γ.

$$I = -\oint_{c_\epsilon(0)} dz \frac{1}{1+z} \frac{f(z)}{z} - \oint_{c_\epsilon(-1)} dz \frac{1}{1+z} \frac{f(z)}{z} + \oint_{c_{1/R}(0)} dt \frac{1}{1+t} f(1/t)$$

$$= -2\pi i \left(\text{res}_{z=0} \left(\frac{1}{1+z} \frac{f(z)}{z} \right) + \text{res}_{z=-1} \left(\frac{1}{1+z} \frac{f(z)}{z} \right) - \text{res}_{z=0} \left(\frac{1}{1+z} f(1/z) \right) \right)$$

$$= -2\pi i (f(0) - f(-1) - \lim_{z\to 0}(z f(1/z)))$$

$$= 2\pi i \left(-\sqrt{-\frac{\omega_-^2}{4}} + \sqrt{-\left(\mu_k^2 + \frac{1}{4}(\omega_+ - \omega_-)^2 \right)} + \sqrt{-\frac{\omega_+^2}{4}} \right). \tag{D7}$$

To compute the square roots we need to specify their phases. This is easily done looking at the Riemann sheet. Indeed, if we look at the real axis, on $z < z_-$ the phase of f^2 is 3π (modulo 4π) so that $f(x) = -i|f(x)|$ for $x = 0$, -1. For the last root, we note that

$$\lim_{z\to 0} z f(1/z) = \lim_{z\to\infty} f(z)/z$$

and because the monodromy of $z = \infty$ is trivial [the phase of $f(z)$ does not change (modulo 2π) if $|z|$ is very large and $\arg(z)$ varies by a period], $z = \infty$ is indeed a pole (and not a branch point) and this limit does not depend on the phase of z. Thus, we can compute it along the positive real axis. But there, the phase of $f(z)^2$ for $z > z_+$ is π, so that $f(z) = i|f(z)|$, and finally we have

$$I = 2\pi i \left(-\left(-i\frac{|\omega_-|}{2} \right) + \left(-i\sqrt{\mu_k^2 + \frac{1}{4}(\omega_+ - \omega_-)^2} \right) \right.$$
$$\left. + i\frac{|\omega_+|}{2} \right)$$

$$= 2\pi \left(\sqrt{\mu_k^2 + \frac{1}{4}(\omega_+ - \omega_-)^2} - \frac{1}{2}(|\omega_+| + |\omega_-|) \right). \tag{D8}$$

Note that in the physically interesting case, that is when $\omega_+ \omega_- < 0$, we have $|\omega_+| + |\omega_-| = |\omega_+ - \omega_-|$ which does not depend on ω, and reproduces exactly (49).

It remains only to check the particular cases, which are however easily obtained by direct integration. For ex-

ample, for $\omega_- = 0$ so that $\omega_+ = 2eQB/A$, we have

$$I/2 = \int_{\text{barrier}} \sqrt{Z_\omega} dx = \frac{1}{2} \int_0^{4(\mu_k^2/\omega_+^2)} \frac{dz}{1+z} \sqrt{\frac{4}{z}\mu_k^2 - \omega_+^2}. \tag{D9}$$

Introducing the new integration variable $s^2 = \frac{4}{z}\mu_k^2 - \omega_+^2$, we get

$$I/2 = \int_0^\infty \left[\frac{1}{\omega_+^2 + s^2} - \frac{1}{4\mu_k^2 + \omega_+^2 + s^2} \right] s^2 ds$$

$$= \int_0^\infty \left[-\frac{\omega_+^2}{\omega_+^2 + s^2} + \frac{4\mu_k^2 + \omega_+^2}{4\mu_k^2 + \omega_+^2 + s^2} \right] ds$$

$$= -\frac{\pi}{2}|\omega_+| + \pi\sqrt{\mu_k^2 + \frac{1}{4}\omega_+^2}.$$

For $\omega_+ = 0$ ($\omega_- = -2eQB/A$) we have

$$I/2 = \int_{\omega_-^2/4\mu_k^2}^\infty \frac{1}{z(1+z)} \sqrt{\mu_k^2 z - \frac{\omega_-^2}{4}}$$

$$= \frac{1}{2} \int_0^{4(\mu_k^2/\omega_-^2)} \frac{dt}{1+t} \sqrt{\frac{4}{t}\mu_k^2 - \omega_-^2},$$

where we used the change of variable $t = 1/z$, obtaining the same integral as in (D9) with ω_- in place of ω_+, giving thus the same result, being $|\omega_\pm| = 2|eQB/A|$.

[1] G. W. Gibbons and S. W. Hawking, Phys. Rev. D **15**, 2738 (1977).
[2] F. Finster, J. Smoller, and S. T. Yau, J. Math. Phys. (N.Y.) **41**, 2173 (2000).
[3] F. Finster, N. Kamran, J. Smoller, and S. T. Yau, Commun. Pure Appl. Math. **53**, 902 (2000); **53**, 1201(E) (2000).
[4] M. Winklmeier and O. Yamada, J. Math. Phys. (N.Y.) **47**, 102503 (2006).
[5] D. Batic and H. Schmid, Prog. Theor. Phys. **116**, 517 (2006).
[6] F. Belgiorno and S. L. Cacciatori, arXiv:0803.2496.
[7] G. Gibbons, Commun. Math. Phys. **44**, 245 (1975).
[8] I. B. Khriplovich, Phys. Rep. **320**, 37 (1999).
[9] W. Heisenberg and H. Euler, Z. Phys. **98**, 714 (1936), English translation in arXiv:physics/0605038.
[10] J. Schwinger, Phys. Rev. **82**, 664 (1951).
[11] S. P. Gavrilov, D. M. Gitman, and J. L. Tomazelli, Nucl. Phys. **B795**, 645 (2008).
[12] S. P. Kim and Don N. Page, Phys. Rev. D **65**, 105002 (2002); **73**, 065020 (2006); **75**, 045013 (2007); Nuovo

Cimento Soc. Ital. Fis. B **120**, 1193 (2005).

[13] S. P. Kim, H. K. Lee, and Y. Yoon, Phys. Rev. D **78**, 105013 (2008).

[14] D. Christodoulou and R. Ruffini, Phys. Rev. D **4**, 3552 (1971).

[15] T. Damour, in *Proceedings of the First Marcel Grossmann Meeting on General Relativity (Trieste, 1975)*, edited by R. Ruffini (North-Holland, Amsterdam, 1977), p. 459.

[16] N. Deruelle, in Proceedings of the First Marcel Grossmann Meeting on General Relativity (Trieste, 1975) (Ref. [15]), p. 483.

[17] N. Deruelle and R. Ruffini, Phys. Lett. **52B**, 437 (1974).

[18] F. Belgiorno and S. L. Cacciatori, Classical Quantum Gravity **25**, 105013 (2008).

[19] S. W. Hawking and Don N. Page, Commun. Math. Phys. **87**, 577 (1983).

[20] A. Bachelot, Commun. Math. Phys. **283**, 127 (2008).

[21] R. A. Konoplya and A. Zhidenko, Phys. Rev. D **76**, 084018 (2007).

[22] F. Belgiorno and S. L. Cacciatori, J. Phys. A **42**, 135207 (2009).

[23] M. Soffel, B. Müller, and W. Greiner, J. Phys. A **10**, 551 (1977).

[24] D. R. Brill and J. A. Wheeler, Rev. Mod. Phys. **29**, 465 (1957).

[25] M. Soffel, B. Müller and W. Greiner, Phys. Rep. **85**, 51 (1982); I. E. Ansdrushkevich and G. V. Shishkin, Theor. Math. Phys. **70**, 204 (1987).

[26] B. Thaller, *The Dirac Equation* (Springer-Verlag, Berlin, 1992).

[27] J. Weidmann, *Spectral Theory of Ordinary Differential Operators*, Lecture Notes in Mathematics Vol. 1258 (Springer-Verlag, Berlin, 1987).

[28] B. S. Kay, Commun. Math. Phys. **100**, 57 (1985).

[29] F. Belgiorno and M. Martellini, Phys. Lett. B **453**, 17 (1999).

[30] F. Belgiorno, Phys. Rev. D **58**, 084017 (1998).

[31] D. B. Hinton and J. K. Shaw, Quart. J. Math. Oxford **36**, 183 (1985).

[32] R. B. Mann and S. F. Ross, Phys. Rev. D **52**, 2254 (1995).

[33] R. Bousso, Phys. Rev. D **60**, 063503 (1999).

[34] W. Pauli, Helv. Phys. Acta **5**, 179 (1932).

[35] S. I. Rubinow and J. B. Keller, Phys. Rev. **131**, 2789 (1963).

[36] L. J. Romans, Nucl. Phys. **B383**, 395 (1992).

[37] F. Belgiorno, S. L. Cacciatori, and F. Dalla Piazza (unpublished).

[38] B. S. Kay and R. M. Wald, Phys. Rep. **207**, 49 (1991).

[39] S. P. Kim, H. K. Lee, and Y. Yoon, Phys. Rev. D **79**, 045024 (2009).

[40] S. P. Kim and H. K. Lee, Phys. Rev. D **76**, 125002 (2007).

[41] M. S. P. Eastham, *The Asymptotic Solution of Linear Differential Systems. Applications of the Levinson theorem*, London Mathematical Society Monographs New Series 4 (Clarendon Press, Oxford, 1989).

[42] Orientation changes because $\arg(1/z) = -\arg z$.